

Fig. 1 Comparison of sphere drag from wind tunnel force balance (t) and wind tunnel free flight (tff) measurements with range free flight (ff) measurements.

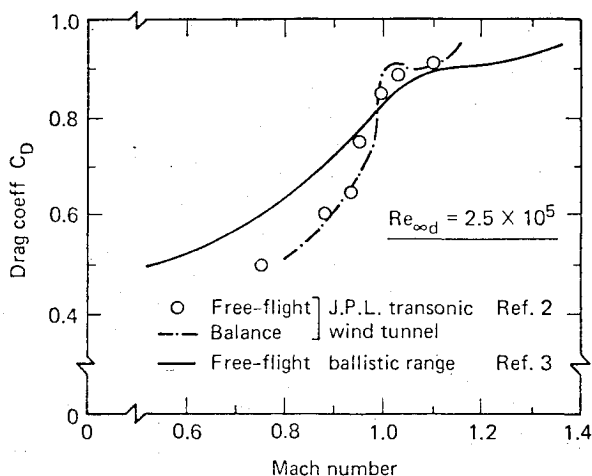


Fig. 2 Summary of sphere drag measurements at high Reynolds numbers in the transonic speed regime.

wind tunnel values of sphere drag coefficient are lower by approximately 15% or more than the free-flight values. It is suggested that this difference indicates that tunnel measurements of sphere drag are affected by wall interference effects. Further verifications of this suggestion could be determined by conducting an additional series of wind tunnel sphere tests using larger and smaller models than those which have already been tested, and comparing the results with existing free-flight data.<sup>3</sup>

It has been shown above that it is possible to use the known value of sphere drag coefficient to evaluate the effect of wall interference on sphere drag measurements in a conventional transonic wind tunnel. In order to apply the same technique to evaluate the performance of a cryogenic transonic wind tunnel it would be necessary 1) to know the variation of sphere drag coefficient in the transonic speed regime for Reynolds numbers on the order of  $10^7$ , and 2) to be able to make sting-free measurements of sphere drag in the tunnel. An analysis of some 19th Century cannon firings by Miller and Bailey<sup>3</sup> has provided values of sphere drag coefficient over much of the required Mach and Reynolds number range of interest (see Fig. 2). Also, Kilgore<sup>1</sup> has indicated that the Langley cryogenic transonic wind tunnel will have a magnetic suspension and balance system which could be used to make the sting-free measurements. Therefore, the possibility does

(or will) exist to evaluate the effects of wall interference and/or condensation on sphere drag measurements in a cryogenic transonic wind tunnel.

It should be noted, however, that there are some Mach number-Reynolds number regions which are relevant to wind tunnel calibrations, but which need further experimental exploration. These are the regions on the right-hand portion of Fig. 2 that contains the particularly interesting dips and maxima at high Reynolds number below and near sonic velocity. These striking features deserve a systematic investigation. The appropriate data could be obtained from a relatively modest experimental program using modern equipment.

### Acknowledgment

Work performed under the auspices of the U.S. Department of Energy by the Lawrence Livermore National Laboratory under Contract W-7405-ENG-48.

### References

- <sup>1</sup>Kilgore, R. A., "Design Features and Operational Characteristics of the Langley 0.3-meter Transonic Cryogenic Tunnel," NASA TND-8304, Dec. 1976.
- <sup>2</sup>Jaffe, P., "A Free-Flight Investigation of Transonic Sting Interference," Jet Propulsion Laboratory, TM 33-704, Jan. 1975.
- <sup>3</sup>Miller, D. G. and Bailey, A. B., "Sphere Drag at Mach Numbers from 0.3 to 2.0 at Reynolds Numbers Approaching  $10^7$ ," *Journal of Fluid Mechanics*, Vol. 93, 1979, pp. 449-464.
- <sup>4</sup>Giraud, M., "Contribution a l'étude de la sphere en transsonique. lère partie: Trainée," Note Technique T11/66, Institute Franco-Allemand de Recherches de St. Louis, St. Louis, France, 1966.
- <sup>5</sup>Zahn, A. F., "Resistance of the Air at Speeds Below One Thousand Feet a Second," *Philosophical Magazine* (Series 6), Vol. 1, 1901, pp. 530-535.

AIAA 81-4039

## Pressure Fluctuations in Transonic Shock-Induced Separation

S. Raghunathan\*

Queen's University, Belfast, Northern Ireland  
and

J. B. Coll†

Rolls-Royce Ltd., Derby, England

### Nomenclature

$c$	= chord length
$f$	= frequency, Hz
$F(n)$	= contribution of $\bar{p}^2/q^2$ in frequency bandwidth $\Delta n$
$\sqrt{nF(n)}$	= $\bar{p}/q(\epsilon)^{1/2}$
$h$	= height of wind-tunnel test section
$\ell_B$	= length of separation bubble
$M$	= Mach number
$M_p$	= peak Mach number
$n$	= frequency parameter based upon test section height, $fh/U_\infty$
$\bar{p}$	= root mean square of static pressure fluctuations
$q$	= upstream dynamic pressure, $\frac{1}{2}\rho U_\infty^2$

Received July 7, 1980. Copyright © American Institute of Aeronautics and Astronautics, Inc., 1980. All rights reserved.

\*Lecturer, Dept. of Aeronautical Engineering.

†Compressor Research Engineer. Member AIAA.

$R_\theta$	= Reynolds number based upon momentum thickness, $U\theta/\nu$
$R_c$	= Reynolds number based upon chord length, $Uc/\nu$
$U_\infty$	= upstream velocity
$U_l$	= local freestream velocity
$\bar{u}$	= root mean square of local velocity fluctuations
$x$	= distance from leading edge of model
$x_s$	= shock position
$\epsilon$	= analyzer bandwidth ratio, $\Delta f/f$
$\theta$	= boundary layer momentum thickness
$\rho$	= density
$\nu$	= kinematic viscosity

### Introduction

It has been observed by the authors<sup>1</sup> that for the case of a shock-induced separation of the steady flow on a 9% maximum thickness half double-wedge airfoil mounted on a wind tunnel roof, the shock position, the pressure, and the velocity profiles in the separated region are substantially unaffected by the tunnel freestream noise in the range  $\bar{p}/q \approx 0.01-0.015$  for  $0.775 < M < 0.80$ . This Note presents the pressure fluctuations on the surface of the model for this range of tunnel freestream noise levels.

### The Tests

Brief details of the test facility and the experimental techniques were presented in earlier reports.<sup>1,2</sup> Pressure fluctuation levels on the surface of the model were measured for a fixed shock position of  $x_s/c = 0.87$  for two levels of freestream tunnel noise,  $\bar{p}/q = 0.010$  and  $0.015$ . The shock strength was sufficient to cause the flow to separate at the shock position, reattaching further downstream of the model on the tunnel roof. The nominal freestream Mach number was 0.78 and the Reynolds number  $R_\theta$  at the leading edge of the model was about  $10^4$ . Kistler type 6503 miniature transducers were mounted upstream, at the shock position, at the trailing edge of the model, and at a distance  $1.25c$  downstream of the trailing edge. The transducers were mounted 1 mm below a 2 mm diam tapping normal to the surface. Flow visualization by the china clay technique insured that the transducers were located in the two-dimensional flow region in the center portion of the model.

### Results

The broadband pressure fluctuation levels measured on the model surface, together with those measured upstream and downstream of the model for the above-mentioned test conditions, are shown in Fig. 1. The maximum pressure fluctuation levels do not occur at the shock position. This suggests that either the shock oscillations are absent or if present they are weak oscillations. The test conditions correspond to a freestream Mach number of 0.78 and  $R_c = 3 \times 10^6$ . McDevitt et al.<sup>3</sup> have shown on a symmetrical airfoil at zero angle of attack that these test conditions would be outside the region of shock oscillations. The peak pressure fluctuations occur in the separated region but not near the reattachment as observed by Mabey.<sup>4</sup> However the number of transducers in the present test are insufficient to locate the peak levels precisely.

The peak Mach number at the shock is  $M_p = 1.55$ . The maximum levels of pressure fluctuations represent only 4% of the mean pressure rise at the shock. This ratio is typically about 20% for separations involving shock oscillations in a supersonic flow<sup>5</sup> and a transonic diffuser flow involving strong separation.<sup>6</sup> The noise level upstream of the shock/boundary-layer interaction region remains constant despite changes in the test section configuration. This is expected as the major source of noise in transonic tunnels is the mixing section downstream of the test section and its propagation upstream is attenuated by the presence of the shock. The change in the tunnel noise, however, produces change in the pressure fluctuation levels in the separated layer

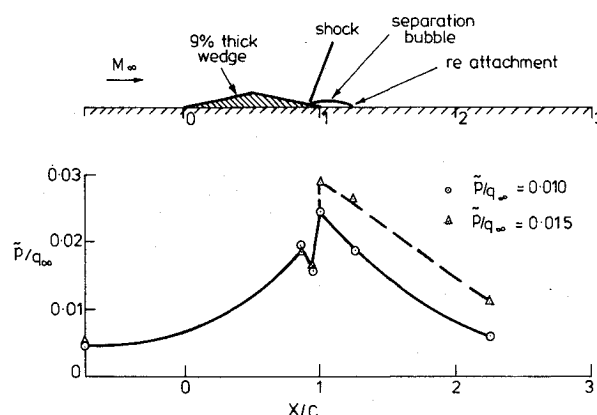


Fig. 1 Broadband pressure fluctuation levels on model.

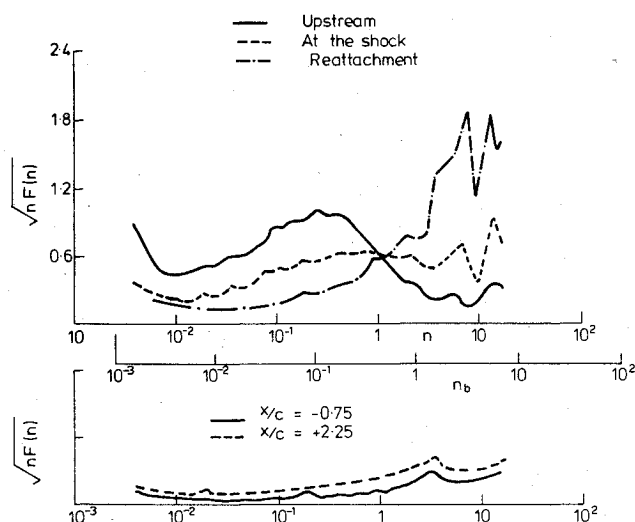


Fig. 2 Turbulence profiles at trailing edge.

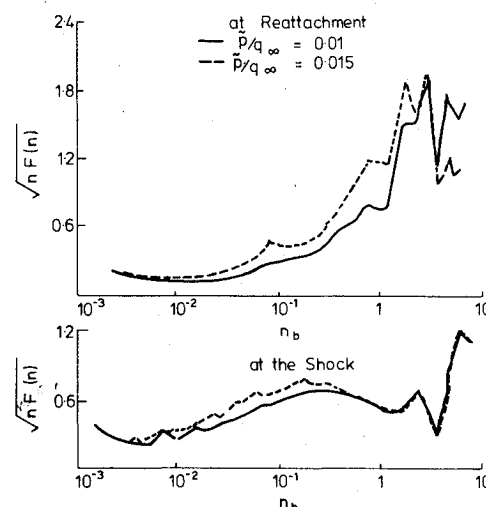


Fig. 3 Spectra of pressure fluctuation in region of shock/boundary-layer interaction.

downstream of the shock. The peak pressure fluctuation levels represent an amplification factor of 5 based upon the upstream conditions and 3-5 based upon the downstream conditions in the tunnel.

Figure 2 shows the turbulence profiles of the separated layer at the trailing edge of the model nondimensionalized with respect to the freestream velocity. Comparison can be made with the profile for an attached turbulent boundary

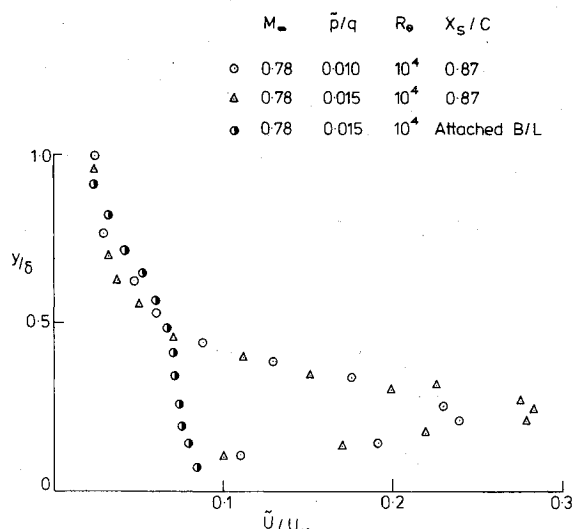


Fig. 4 Influence of tunnel noise on pressure fluctuation spectra.

layer at the same freestream Mach number and with  $\bar{p}/q_\infty \approx 0.015$ . The turbulence intensity levels in the separated layer indicate an amplification factor of 3-4 which is of the same order as that for the pressure fluctuation levels. It is observed that there are no significant changes in the turbulence levels with the change in the tunnel noise level from  $\bar{p}/q_\infty = 0.010$  to 0.015. The freestream level of turbulence is unaffected by separation and change in the tunnel noise.

The spectra of pressure fluctuation in the region of shock/boundary-layer interaction for a tunnel noise level  $\bar{p}/q_\infty = 0.01$  are shown in Fig. 3. The increase in pressure fluctuation levels in the separated region essentially occur at higher frequencies. The peak frequencies shift progressively across the shock. The peak frequency based upon the separation bubble length is  $n_b = 2$ . The peak frequencies based upon the chord length occur at  $n \approx 4$  with harmonics at  $n \approx 8$  and  $n \approx 12$ . The peak frequencies upstream and downstream of the interaction ( $x/c = -0.75$  and  $2.25$ ) are also  $n \approx 4$ . This suggests a correlation between the tunnel noise and the pressure fluctuation levels in the separated layer.

As shown in Fig. 4, changes in the wind-tunnel test section configuration to produce different noise levels have an effect on the pressure fluctuation spectra within the region of shock/boundary-layer interaction but do not effect the length of the separation bubble.

### Acknowledgment

This work originated as part of the research supported by the Science Research Council contract GR/A/53772. The help from the Aeronautical Engineering workshop is greatly appreciated.

### References

- <sup>1</sup>Raghuathan, S., Coll, J. B., and Mabey, D. G., "Flat Plate Turbulent Boundary Layers Subjected to Large Pressure Fluctuations," *AIAA Journal*, Vol. 17, Jan. 1979, pp. 105-107.
- <sup>2</sup>Raghuathan, S., Coll, J. B., and Mabey, D. G., "Transonic Shock/Boundary Layer Interaction Subjected to Large Pressure Fluctuations," *AIAA Journal*, Vol. 17, Dec. 1979, pp. 1404-1406.
- <sup>3</sup>McDevitt, J. B., Levy, L. L., Jr., and Deiwert, G. S., "Transonic Flow about a Thick Circular-Arc Airfoil," *AIAA Journal*, Vol. 14, May 1976, pp. 606-613.
- <sup>4</sup>Mabey, D. G., "Analysis and Correlation of Data on Pressure Fluctuations in Separated Flow," *Journal of Aircraft*, Vol. 9, Sept. 1972, pp. 642-645.
- <sup>5</sup>Plotkin, K. J., "Shockwave Oscillations Driven by Turbulent Boundary Layer Fluctuations," *AIAA Journal*, Vol. 13, Aug. 1975, pp. 1036-1040.
- <sup>6</sup>Chen, C. P., Sajben, M., and Kroutil, J. C., "Shockwave Oscillations in a Transonic Diffuser Flow," *AIAA Journal*, Vol. 17, Oct. 1979, pp. 1076-1083.

AIAA 81-4040

## Algorithm for Rapid Integration of Turbulence Model Equations on Parabolic Regions

David C. Wilcox\*

DCW Industries, Inc., Studio City, Calif.

### Introduction

THE advent of advanced engineering models of turbulence such as those described by Launder and Spalding<sup>1</sup> has been accompanied by a need for advanced numerical methods. For most of these advanced models, conventional numerical methods often are quite difficult to apply and sometimes do not work at all. For example, for a relatively simple flow such as fully developed channel flow explicit time-marching algorithms, relaxation schemes and the shooting method fail to yield a converged solution. The purpose of this Note is to cite yet another occasion where integration of an advanced set of turbulence-model equations has been unusually difficult and to describe the resolution of the problems encountered.

While developing a three-dimensional boundary-layer program using a standard parabolic marching scheme, the author has found computing time with the Wilcox-Rubesin<sup>2</sup> two-equation turbulence model to be very lengthy. The long computing time occurs because converged solutions are possible only when very small streamwise steps are taken. This observation is consistent with results obtained by Rastogi and Rodi<sup>3</sup> who have devised a three-dimensional boundary-layer program which uses the Jones-Launder<sup>4</sup> two-equation turbulence model. Rastogi and Rodi find that their initial stepsize  $\Delta s$  must be of the order of 1/100th of the local boundary-layer thickness  $\delta$  and that ultimately  $\Delta s$  generally cannot exceed  $\delta/2$ . By contrast, a typical mixing-length computation for a three-dimensional wing begins with  $\Delta s/\delta \sim 4$  and maintains a  $\Delta s/\delta$  ratio in excess of unity. Such a severe stepsize limitation would increase computing time over that required for the mixing-length model by a factor of 10-100, depending upon the ultimate Reynolds number. Even if such run times were tolerable, the computer storage requirements for a real airplane wing would be prohibitive. Clearly an innovation is needed. The next section presents the necessary innovation.

### Analysis

#### Model Equations

To illustrate the essence of the problems encountered while integrating turbulence-model equations, we begin by casting the turbulent energy equation in discretized form for a *two-dimensional* boundary layer. For the Wilcox-Rubesin model the differential equation for turbulent energy  $e$  is

$$u \frac{\partial e}{\partial s} + v \frac{\partial e}{\partial y} = \gamma^* \frac{(\partial u / \partial y)^2}{\omega} e - \beta^* \omega e + \frac{\partial}{\partial y} \left\{ (\nu + \sigma^* \epsilon) \frac{\partial e}{\partial y} \right\} \quad (1)$$

where  $s$  is arclength along the body,  $y$  the distance normal to the surface,  $u$  and  $v$  the velocity components in the  $s$  and  $y$  directions, and  $\omega$  the turbulent dissipation rate. The quantities  $\nu$  and  $\epsilon$  denote kinematic molecular and eddy viscosity, respectively, while  $\gamma^*$ ,  $\beta^*$ , and  $\sigma^*$  are closure coefficients whose values have been empirically found to be 1, 9/100, and

Received July 15, 1980. Copyright © American Institute of Aeronautics and Astronautics, Inc., 1980. All rights reserved.

\*President, Associate Fellow AIAA.